EXTENSION OF WINDING FUNCTION THEORY FOR RADIAL AND AXIAL NON-UNIFORM AIR GAP IN SALIENT POLE SYNCHRONOUS MACHINES

H. Akbari

Department of Electrical Engineering
Science and Research Branch
Islamic Azad University, Tehran, Iran

H. Meshgin-Kelk

Department of Electrical Engineering
Tafresh University, Tafresh, Iran

J. Milimonfared

Department of Electrical Engineering
Amirkabir University of Technology, Tehran, Iran

Abstract—In this paper, to calculate the salient pole machine inductances under radial and axial non-uniformity, a new method is developed. The method, an extension of the modified winding function theory to 3D, allows studying salient pole machines with radial and axial non-uniform air gap considering more realistic mean radius of the air gap. By using the developed method and a precise geometrical model, inductances of a salient pole machine with inclined rotor are calculated. Inductances are evaluated and effects of several asymmetries on inductances are shown. Calculated inductances are used in a coupled electromagnetic model, for simulation of a salient pole machine under healthy and different inclined eccentricity conditions. Simulation results show that the 19th stator current harmonic can be detected to alarm for inclined rotors. Experimental results that validate the theoretical and simulation results are presented.

1. INTRODUCTION

Approximately 80% of the mechanical faults lead to the non-uniformity between rotor and stator [1]. Relatively small amount of unequal air-gap can have a significant impact on the operational life of bearings. Machine eccentricity is the condition of unequal air gap that exists between the stator and rotor. Static eccentricity (SE) occurs when the rotor rotates about its own center but this center does not coincide with that of the stator. In this case, the position of the minimal radial air gap length is fixed in space. Dynamic eccentricity (DE) occurs when the rotor geometric center is not at the center of rotation and the position of minimum air gap rotates with the rotor. In reality, static and dynamic eccentricities tend to coexist [2]. In these conditions, the air gap length changes in radial direction and the rotor axis is parallel to that of the stator. Therefore the machine is uniform axially.

Inclined or axial eccentricity occurs when the axis of rotor is not parallel to the stator axis. In this type of misplaced rotor fault, along the axial direction, the eccentricity level is not constant. This fault may caused by improper alignment of right and left bearings centers, centrifugal phenomena, oscillation of connected load to the shaft, shaft deflection due to thermal distortions or externally imposed misaligning moments [3]. Inclined eccentricity fault has been analyzed in other motors and applications such as [3, 4], while this analysis has not been considered for application in salient pole synchronous machine, and this paper is an attempt to achieve that purpose.

Generally, three approaches have been used for modeling and detection of faults in electrical machines: magnetic equivalent circuit method (MECM), finite element method (FEM) and winding function method (WFM). The MECM needs shorter computation time compared with the FEM, but it is less accurate. In this method, the directions of the magnetic flux lines must be known [5]. Studying faulty electrical machines needs precise mathematical models and MECM is not capable to diagnose the fault in the real cases [1, 6]. Although, FEM gives accurate results, however, this method is time consuming especially for the analysis of electrical machines with asymmetry in the motor body such as air gap eccentricity. Moreover it requires an extensive characterization of the machine, for example, electromagnetic properties of all the materials making up the machine and the physical geometry [1, 7–10].

In this paper, for analysis of salient pole machines under inclined eccentricity conditions, winding function theory is extended to 3D and more precise geometrical model of machine under these conditions is presented. Winding function theory is based on the basic geometry

and winding layout of machine [11]. An essential part of this theory is the calculation of machine inductances. These inductances are evaluated using winding function and other equations within the theory. The only information required in winding function approach is the winding layout and machine geometry. By this approach, it is possible to analyze performance of any faulty machine with any type of winding distribution and air gap distribution around rotor, while taking into account all spatial and time harmonics. Hence this method has found application in the analysis of asymmetrical and fault conditions in machines, Such as broken rotor bars [12, 13] and fault condition in stator windings [14, 15]. The modified winding function approach (MWFA) for asymmetrical air-gap in a salient pole synchronous machine has been proposed in [16]. This modification was later more developed for non-uniform air gap machines [17, 18]. This theory has been applied to analyze static, dynamic and mixed eccentricity in induction and synchronous machines [4, 19–22]. Some techniques were also developed to include rotor bars skewing effect [23], slotting effect [24], saturation effect [25] and inter-bar currents [26] in the model.

In the previous works, based on winding function theory, the analysis of salient pole machines performance under eccentricity conditions is carried out assuming uniformity down the axial length of the machine. In the other hand, the rotor axis is considered to be parallel to that of the stator. Thus the objective of this paper is to develop a method for salient pole machine analysis under inclined eccentricity conditions. The extended method allows taking into account radial and axial non-uniformity effects without assuming uniform mean radius of the air gap. The paper will in particular treat how radial and axial non-uniformities can be modeled in the actual space using winding function theory. In order to have a pure problem, several other physical problems such as leakage flux and magnetic saturation are not included in this paper; they will be included in future work.

The contributions of the present paper includes: 1). Developing a new method for calculation of salient pole machine inductances under radial and axial nonuniformity conditions, based on winding unction theory, 2). Introducing a precise geometrical model of salient pole machines under different axial eccentricity conditions, 3). Analyzing the detectability of the inclined eccentricity in a salient pole synchronous machine through motor current signature analysis (MCSA).

2. EXTENSION OF THE WINDING FUNCTION THEORY

To obtain the equation for the inductance computation, an elementary four pole salient pole synchronous machine scheme is presented in Fig. 1.
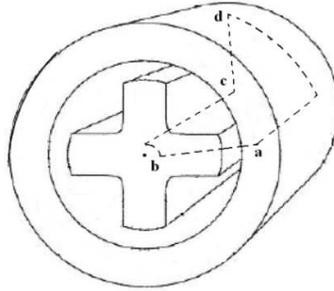
Figure 1. An elementary salient pole machine.

The stator shape is assumed to be cylindrical. Also the permeability of the stator and rotor iron cores is assumed to be infinite when compared to the permeability of the air gap. There are no restrictions about windings distribution for the analysis. Furthermore, restrictions over the air-gap eccentricity are not assumed. Then the machine can exhibit radial and axial non-uniformity.

The stator reference position of the closed path, *abcda* of Fig. 1, the angle φ, is taken at an arbitrary point along the air gap. Points b and c are located on the rotor and points a and d are located on the stator. Points a, b are located in $\varphi = 0$ and $z = 0$ and Points c, d are located in φ and z. Considering the closed path *abcda* of Fig. 1 for an arbitrary $0 < \varphi < 2\pi$ and $0 < z < l$ and applying the Ampere's law over the closed path, the following relation can be obtained.

$$\oint \mathbf{H}\left(\varphi, z, \theta\right) \cdot d\mathbf{l} = \int \mathbf{J} \cdot d\mathbf{s} \tag{1}$$

where, H is magnetic field intensity, J is current density, φ is arbitrary angle in stator reference frame, θ is rotor position angle in stator reference frame, S is a surface enclosed by *abcd* and l is the axial stack length of the machine. Since all of the windings enclosed by the closed path carry the same current i, (1) results as follows:

$$\oint \mathbf{H}\left(\varphi, z, \theta\right) \cdot d\mathbf{l} = n\left(\varphi, z, \theta\right) i \tag{2}$$

The function $n(\varphi, z, \theta)$ represents the number of the winding turns enclosed by the closed path. Turns carrying currents i into the page are considered positive and while the turns carrying currents i out of the page are considered negative. In terms of MMF drops in a magnetic circuit, (2) can be written as

$$F_{ab}(0,0,\theta) + F_{bc}(\varphi, z, \theta) + F_{cd}(\varphi, z, \theta) + F_{da}(\varphi, z, \theta) = n(\varphi, z, \theta) i \quad (3)$$

The relative permeability of the stator and rotor iron cores is considerably larger than that of the air gap. Therefore the MMF drops across the iron, F_{bc}, F_{da} are negligible and (3) reduces to

$$F_{ab}(0,0,\theta) + F_{cd}(\varphi, z, \theta) = n(\varphi, z, \theta) \cdot i \quad (4)$$

Dividing (4) by the air-gap function (g), and multiplying by the mean radius function (r) and finally integrating it with respect to the φ between $0 - 2\pi$ and z between $0 - l$ yields

$$\int_0^{2\pi} \int_0^l \frac{r(\varphi, z, \theta) F_{ab}(0,0,\theta)}{g(\varphi, z, \theta)} dz d\varphi + \int_0^{2\pi} \int_0^l \frac{r(\varphi, z, \theta) F_{cd}(\varphi, z, \theta)}{g(\varphi, z, \theta)} dz d\varphi$$

$$= \int_0^{2\pi} \int_0^l \frac{r(\varphi, z, \theta) n(\varphi, z, \theta) i}{g(\varphi, z, \theta)} dz d\varphi \quad (5)$$

For $F_{ab}(0,0,\theta)$ calculation, Gauss's law for magnetic field can be used.

$$\oint_S \mathbf{B} \cdot d\mathbf{s} = 0 \quad (6)$$

where B is the magnetic flux density and $\mathbf{s}$ is a closed surface of radius $r(\varphi, z, \theta)$, placed exactly between the rotor and the stator surfaces.

$$\int_0^{2\pi} \int_0^l \mu_0 r(\varphi, z, \theta) H(\varphi, z, \theta) dz d\varphi = 0 \quad (7)$$

where μ_0 is free space permeability. It is known that the magnetic field intensity is the product of the MMF and the inverse air gap function. Thus

$$H(\varphi, z, \theta) = F(\varphi, z, \theta) g^{-1}(\varphi, z, \theta) \quad (8)$$

Replacing (8) in (7) yields

$$\int_0^{2\pi} \int_0^l \frac{r(\varphi, z, \theta) F(\varphi, z, \theta)}{g(\varphi, z, \theta)} dz d\varphi = 0 \quad (9)$$

Then the second term in (5) is equal to zero and (5) will reduce to the following

$$\int_0^{2\pi} \int_0^l \frac{r(\varphi, z, \theta) F_{ab}(0, 0, \theta)}{g(\varphi, z, \theta)} dz d\varphi = \int_0^{2\pi} \int_0^l \frac{r(\varphi, z, \theta) n(\varphi, z, \theta) i}{g(\varphi, z, \theta)} dz d\varphi \quad (10)$$

Therefore

$$F_{ab}(0, 0, \theta) 2\pi l \int_0^{2\pi} \int_0^l r(\varphi, z, \theta) g^{-1}(\varphi, z, \theta) dz d\varphi$$

$$= \int_0^{2\pi} \int_0^l \frac{r(\varphi, z, \theta) n(\varphi, z, \theta) i}{g(\varphi, z, \theta)} dz d\varphi \quad (11)$$

Solving (11) for $F_{ab}(0, 0, \theta)$, this function can be obtained as follows:

$$F_{ab}(0, 0, \theta) = \frac{\int_0^{2\pi} \int_0^l \frac{r(\varphi, z, \theta) n(\varphi, z, \theta) i}{g(\varphi, z, \theta)} dz d\varphi}{2\pi l \int_0^{2\pi} \int_0^l r(\varphi, z, \theta) g^{-1}(\varphi, z, \theta) dz d\varphi} \quad (12)$$

Substituting (12) in (4) and solving for F_{cd} yields

$$F_{cd}(\varphi, z, \theta) = n(\varphi, z, \theta) i - \frac{\int_0^{2\pi} \int_0^l r(\varphi, z, \theta) g^{-1}(\varphi, z, \theta) n(\varphi, z, \theta) i dz d\varphi}{2\pi l \int_0^{2\pi} \int_0^L r(\varphi, z, \theta) g^{-1}(\varphi, z, \theta) dz d\varphi} \quad (13)$$

Dividing (13) by i, the "Extended MWF", $E(\varphi, z, \theta)$, is derived as follows:

$$E(\varphi, z, \theta) = n(\varphi, z, \theta) - \frac{\int_0^{2\pi} \int_0^l r(\varphi, z, \theta) g^{-1}(\varphi, z, \theta) n(\varphi, z, \theta) dz d\varphi}{2\pi l \int_0^{2\pi} \int_0^L r(\varphi, z, \theta) g^{-1}(\varphi, z, \theta) dz d\varphi} \quad (14)$$

$E(\varphi, z, \theta)$ can be defined for each machine winding.

3. DERIVATION OF INDUCTANCES EQUATION

The MMF distribution in the air gap, produced by current i_A of winding A, can simply be found by product of $E_A(\varphi, z, \theta)$ from (14) and the current flowing in the winding.

$$F_A(\varphi, z, \theta) = E_A(\varphi, z, \theta) i_A \quad (15)$$

The differential flux across the gap through a differential area, $r(\varphi, z, \theta) dz d\varphi$, from rotor to stator is as follows:

$$d\varphi = F_A(\varphi, z, \theta) \frac{\mu_0 r(\varphi, z, \theta) dz d\varphi}{g(\varphi, z, \theta)} \quad (16)$$

Integrating the differential flux in the region covered by either a stator coil or rotor coil, yields

$$\varphi_{BA} = \mu_0 \int_{\varphi_1}^{\varphi_2} \int_{z_1}^{z_2} r(\varphi, z, \theta) E_A(\varphi, z, \theta) g^{-1}(\varphi, z, \theta) i_A dz d\varphi \qquad (17)$$

$n_B(\varphi, z, \theta)$ is equal to the coil turns in the region ($\varphi_1 < \varphi < \varphi_2$, $z_1 < z < z_2$) and zero otherwise. Therefore the total flux linking coil B due to current in winding A, λ_{BA}, is obtained from multiplying (17) by $n_B(\varphi, \theta)$ and integrating it over the whole surface.

$$\lambda_{BA} = \mu_0 \int_0^{2\pi} \int_0^l r(\varphi, z, \theta) n_B(\varphi, z, \theta) E_A(\varphi, z, \theta) g^{-1}(\varphi, z, \theta) i_A dz d\varphi \tag{18}$$

The mutual inductance of windings A and B, due to current i_A in the coil A (L_{BA}), is

$$L_{BA} = \frac{\lambda_{BA}}{i_A} \qquad (19)$$

Therefore

$$L_{BA} = \mu_0 \int_0^{2\pi} \int_0^l r(\varphi, z, \theta) n_B(\varphi, z, \theta) E_A(\varphi, z, \theta) g^{-1}(\varphi, z, \theta) dz d\varphi \tag{20}$$

In the same way, mutual inductance between windings B and A, due to current i_B in coil B, can be derived as follows:

$$L_{AB} = \mu_0 \int_0^{2\pi} \int_0^l r(\varphi, z, \theta) n_A(\varphi, z, \theta) E_B(\varphi, z, \theta) g^{-1}(\varphi, z, \theta) dz d\varphi \tag{21}$$

In the inductance equation, the mean radius of the air gap, unlike previous proposals, depends on the geometry of the air gap down the machine axial length. Equations (20) and (21) have cumulative property. Thus the condition of $L_{AB} = L_{BA}$ is always satisfied. This method has capability to simulate the mechanical asymmetry and fault of stator and rotor which has no restrictions about axial and radial non-uniformities. Also space harmonics of the windings MMF and slots harmonics are taken into account in the model.

4. STATIC INCLINED ECCENTRICITY MODELING

Eccentricity of stator and rotor is one of the basic faults in electrical machines. Static eccentricity (SE), Dynamic eccentricity (DE) and mixed eccentricity (ME) lead to a circumferential non-uniform air gap. In these eccentricity faults, the rotor axis is parallel to that of the

stator. The air gap length variation under SE for induction machines can be described by air gap function as follows [23]:

$$g\left(\varphi, \varphi_s, \delta_s\right) = g_0(1 - \delta_s \cos(\varphi - \varphi_s)) \tag{22}$$

where, g_0 is the air gap length, φ_s is the angle at which rotor rotation and stator centers are separated and δ_s is the static eccentricity coefficient. The distance between stator and rotation centers is $g_0\delta_s$.
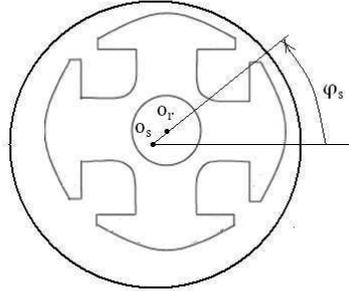
Figure 2. Static eccentricity in an elementary salient pole machine. o_s is stator center and o_r is rotor rotation center.

Figure 2 shows the static eccentricity in an elementary salient pole machine. For salient pole machines, the air gap length variation under SE is as follows:

$$g\left(\varphi, \theta, \varphi_s\right) = g_h\left(\varphi, \theta\right) - D_{sr}\cos\left(\varphi - \varphi_s\right) \tag{23}$$

In (23), $g_h(\varphi, \theta)$ is the air gap function for the healthy salient pole machine and D_{sr} is the distance of stator and rotation centers. As shown in Figure 2, the distance of stator and rotation centers is independent of $g_h(\varphi, \theta)$ or the air gap length above pole shoes (g_p). The static eccentricity coefficient (δ_s) is defined as: D_{sr}/g_p. Therefore

$$\begin{aligned} g\left(\varphi, \theta, \varphi_s, \delta_s\right) &= g_h\left(\varphi, \theta\right) - g_p\delta_s \cos\left(\varphi - \varphi_s\right) \\ &= g_h\left(\varphi, \theta\right) \left(1 - g_p\delta_s g_h^{-1}\left(\varphi, \theta\right) \cos\left(\varphi - \varphi_s\right)\right) \end{aligned} \tag{24}$$

In (24), g_p and $g_h^{-1}(\varphi, \theta)$ are the air gap length above pole shoes and the inverse air gap function for the healthy machine respectively. Stator and rotor slots and the pole saliency can be taken into account by using the techniques introduced in [24, 27].

In the case of the inclined eccentricity, along the axial direction, the degree of eccentricity is not constant and the air gap changes in both axial and radial directions. Then, the original MWFA is not valid to compute the inductances and the extended MWFA has to be used. To model the inclined eccentricity, this fault can be treated as a variable
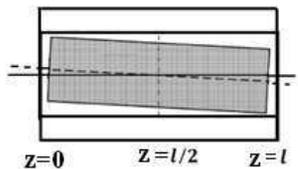
Figure 3. Symmetrical inclined eccentricity.
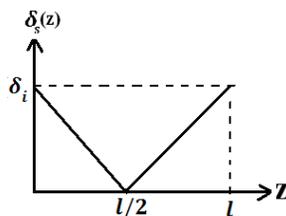
Figure 4. Variation of static eccentricity coefficient for machine with symmetrical inclined eccentricity.

circumferential eccentricity. Fig. 3 shows an elementary machine with symmetrical inclined eccentricity. Symmetrical inclined eccentricity is the eccentricity symmetric to the midpoint of the machine shaft.

Figure 4 shows the variation of static eccentricity coefficient versus position along the axial direction in this condition.

Obviously, the air-gap and the mean radius functions change in non-uniformity conditions compared to the symmetrical conditions. In symmetrical inclined eccentricity, the air-gap function can be represented by

$$g(\varphi,\theta,\varphi_s,z) = g_h(\varphi,\theta)\left(1 - g_p\delta_s(z)\,g_h^{-1}(\varphi,\theta)\cos(\varphi-\varphi_s)\right),\ \ 0 < z < l/2 \tag{25}$$

where

$$\delta_s(z) = \frac{-2\delta_i}{l}\cdot z + \delta_i \tag{26}$$

and

$$g(\varphi,\theta,\varphi_s,z) = g_h(\varphi,\theta)\left(1 - g_p\delta_s(z)\,g_h^{-1}(\varphi,\theta)\cos(\varphi-\varphi_s+\pi)\right),$$
$$l/2 < z < l \tag{27}$$

where

$$\delta_s(z) = \frac{\delta_i(2z-l)}{l} \tag{28}$$

In (28), δ_i is static eccentricity coefficient in front side or back side of the machine. The mean radius function is obtained as follows:

$$r(\varphi,\theta,\varphi_s,z) = r_s(\varphi) - \frac{g(\varphi,\theta,\varphi_s,z)}{2} \tag{29}$$

where, $r_s(\varphi)$ is the inner stator radius of the machine. Mean radius function depends on the geometry of the air gap. In previous studies, this function has been considered to be constant. Fig. 5 shows variation of mean radius of the air gap for the healthy salient pole machine.

Figure 6 shows an elementary machine with asymmetrical inclined eccentricity. The occurrence of asymmetrical inclined eccentricity (solid line) means the separation of the rotor axis from the symmetrical inclined rotor (dotted line). The distance of symmetrical inclined rotor and asymmetrical inclined rotor is $\delta_n g$.

Figure 7 shows the variation of static air gap eccentricity coefficient versus axial position in this condition. As shown, the
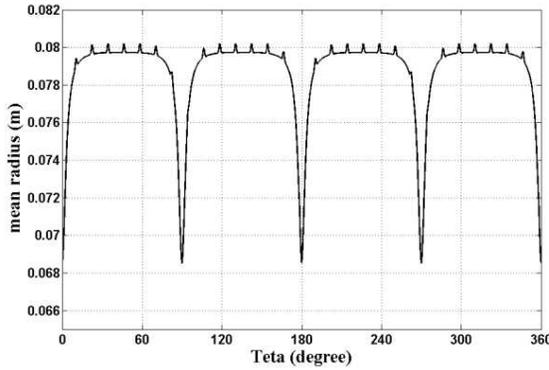
Figure 5. Mean radius function for healthy salient pole machine ($\theta = 0,\ z = 0$).
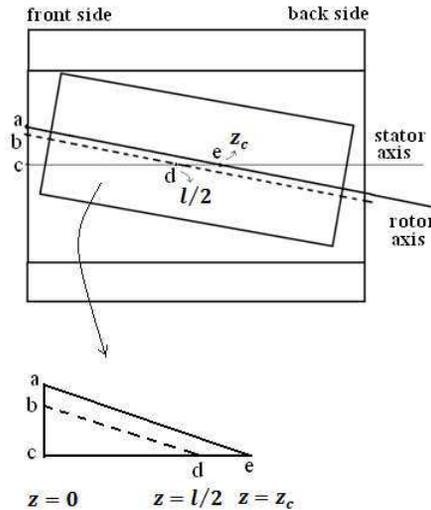
Figure 6. Asymmetrical inclined eccentricity in an elementary machine.
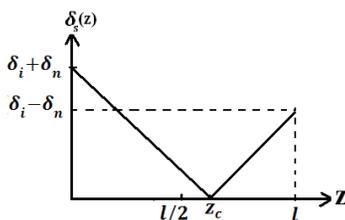
Figure 7. Variation of static eccentricity coefficient in different positions for machine under asymmetrical inclined eccentricity.

eccentricity coefficient in front side and back side of the machine is $(\delta_i + \delta_n)$ and $(\delta_i - \delta_n)$ respectively.

Through geometric analysis on Figs. 6 and 7, the air gap length at any point along the shaft can be represented by

$$g\left(\varphi, \theta, \varphi_s, z\right) = g_h\left(\varphi, \theta\right)\left(1 - g_p \delta_s\left(z\right) g_h^{-1}\left(\varphi, \theta\right)\cos\left(\varphi - \varphi_s\right)\right),$$
$$0 < z < z_c \quad (30)$$

where

$$\delta_s\left(z\right) = \frac{-\delta_n - \delta_i}{z_c} \cdot \left(z - z_c\right) + \delta_i + \delta_n \quad (31)$$

and

$$g\left(\varphi, \theta, \varphi_s, z\right) = g_h\left(\varphi, \theta\right)\left(1 - g_p \delta_s\left(z\right) g_h^{-1}\left(\varphi, \theta\right)\cos\left(\varphi - \varphi_s + \pi\right)\right),$$
$$z_c < z < l \quad (32)$$

where

$$\delta_s\left(z\right) = \frac{\delta_i - \delta_n}{l - z_c} \cdot \left(z - z_c\right) \quad (33)$$

The mean radius function is calculated from (29). A shown in Fig. 6, three-angles ace and bcd are similar. Therefore

$$\frac{z_c}{l/2} = \frac{\left(\delta_i + \delta_n\right)}{\delta_i} \quad (34)$$

where, z_c is the cross section position of stator axis and rotor axis. Solving (34) for z_c yields

$$z_c = \frac{\left(\delta_i + \delta_n\right)l}{2\delta_i} \quad (35)$$

So it is possible to model different types of static inclined eccentricities, without any restriction about axial non-uniformity.

5. INDUCTANCES COMPUTATIONS UNDER DIFFERENT ECCENTRICITY CONDITIONS

In this section, the inductances of a three-phase four pole 9 kVA salient pole synchronous machine are computed under healthy and different eccentricity conditions. Inductances are calculated by means of developed method and proposed geometrical model of machine in this condition. The machine dimension details are given in the Table 1.

The plots of magnetizing inductances of stator and rotor windings and mutual inductance between stator and rotor windings with respect to rotor position along rotor shaft are shown in Fig. 8. It should be noted that the magnetic saturation has not been considered.

Some inductance plots are shown in Figs. 9 and 10. As shown, the magnetizing inductance of the stator phase A and mutual inductance between stator phase A and rotor winding change with rotor position, whereas the magnetizing inductance of the rotor winding is constant. It can be seen that the inductances of salient pole machine under inclined

(a)

(b)

(c)
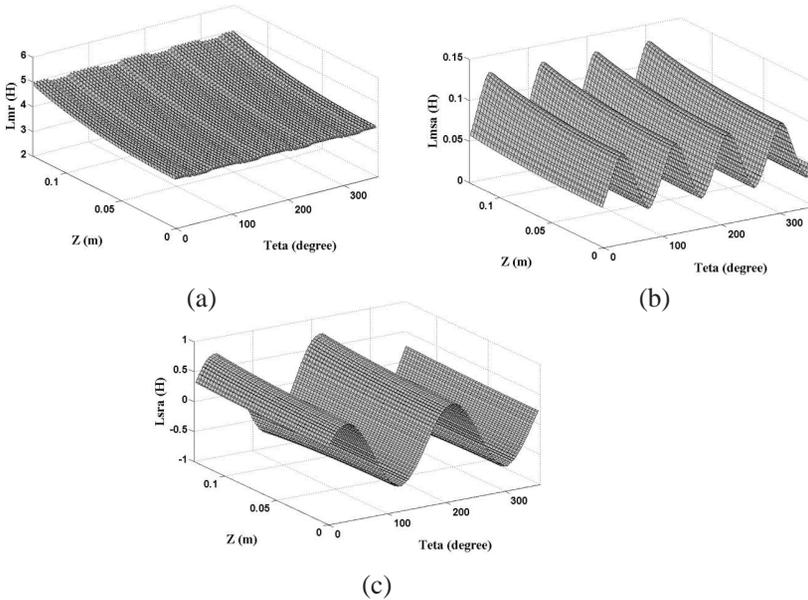
Figure 8. Variation of inductances under inclined eccentricity (one end $(z = 0)$ is 0% and the other end $(z = l)$ is +75%). (a) Magnetizing inductance of rotor winding, (b) magnetizing inductance of stator phase A and (c) mutual inductance between stator phase A and rotor winding.

Table 1. Dimensions of simulated machine.

Pole arc (degrees)	57
Inner radius of stator (mm)	80
Air gap length (mm)	0.6
Active axial length (mm)	130
Number of turns per slot	18
Number of stator slots	30
Stator slot pitch (degrees)	12
Rotor outer radius (mm)	79.4

(a)

(b)

(c)
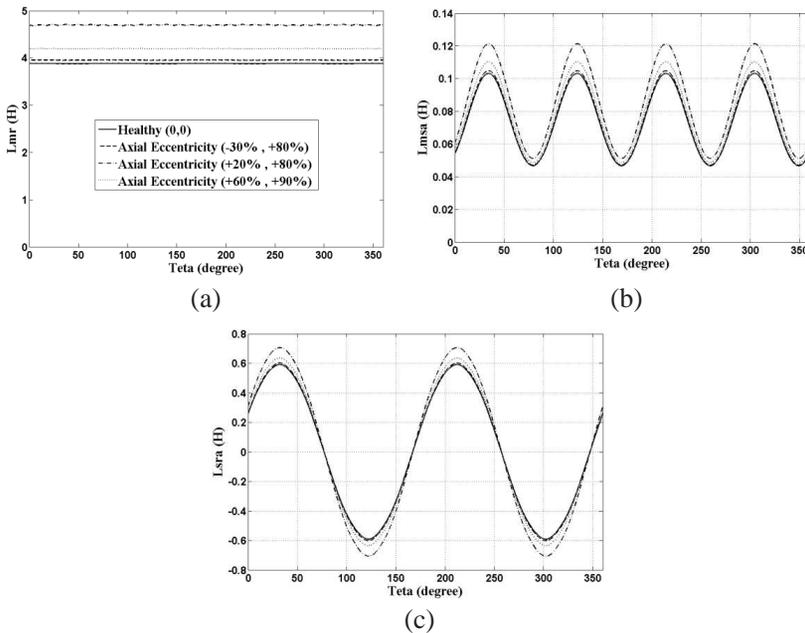
Figure 9. Inductances of the machine under different conditions. (a) Magnetizing inductance of rotor winding, (b) magnetizing inductance of stator phase A and (c) mutual inductance between stator phase A and rotor winding.

eccentricity condition are the average value of inductances along the rotor axis. For example, inductances of a machine with inclined rotor which one end is -30% SE and the other end is 80% SE, is equal to those of machine with a uniform 25% SE.
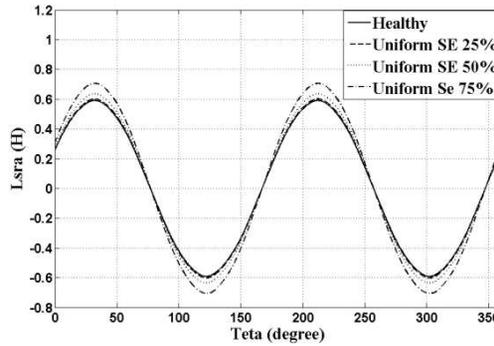
Figure 10. Mutual inductance between stator phase A and rotor winding under different eccentricity conditions.

6. DYNAMIC SIMULATION OF A SALIENT POLE MACHINE

The calculated inductances are used in a coupled electromagnetic model for simulation and studying the frequency spectrum of stator line current in the presence of inclined eccentricity. The fundamental equations of multiple coupled circuit model of the machine are as follows [16]:

$$V_s = \frac{d\lambda_s}{dt} + R_s I_s \tag{36}$$

$$V_r = \frac{d\lambda_r}{dt} + R_r I_r \tag{37}$$

$$T_e - T_l = j\frac{dw}{dt} \tag{38}$$

$$T_e = \frac{\partial w_{co}}{\partial \theta} \tag{39}$$

where
$$w_{co} = I_s^T L_{ss} I_s + I_r^T L_{rr} I_r + I_s^T L_{sr} I_r + I_r^T L_{rs} I_s \tag{40}$$

V, I and λ are voltage, current and flux linkage of windings, T_e is developed electromagnetic torque, T_l is load torque, w_{co} is co-energy and j is the inertia of the rotor. The electromagnetic coupling model of the machine circuits is solved using a 4th and 5th order Runge-Kutta method. The machine used for the simulation and experiment doesn't have damper winding in the rotor. The damper winding which consists of k bars and two end rings can be treated as $k + 1$ loops, which are coupled with each other, with the stator and the field windings, through the mutual inductances. Resistance and inductance matrices

Table 2. Simulated relative percentage increase of stator current harmonics due to different inclined eccentricities under 50% load level.

Harmonic order	(SE degree (%) at two ends)				
	−30 +30	−60 +60	−20 +60	+30 +60	+70 +70
5th	0%	1%	4%	5.5%	8%
7th	0%	1%	5%	6%	9%
11th	0%	1.5%	3%	6%	7.5%
13th	0.5%	1.5%	7%	21%	26%
17th	0%	1%	5%	15%	18%
19th	2%	3%	24%	58%	80%
23th	1%	2%	9%	28%	31%

can be easily obtained by voltage equations in damper loops, field winding and stator phases. The details of damper winding modeling in a synchronous machine have been given in [28].

The frequency spectra of line current are obtained using the Fast Fourier Transform (FFT). Stator current harmonics for different inclined eccentricities under 50% load level have been summarized in Table 2 as percentage values with respect to the healthy machine. It is clear that the 19th stator current harmonic has the highest relative percentage increase. Also the cases with same average SE level show similar component amplitude. Thus the machine current may not be the appropriate one for detecting inclined eccentricities with a low average value.

7. EXPERIMENTAL RESULTS

In order to validate the developed method and the proposed geometrical model of machine, experiments have been performed on a machine identical to the one simulated. To be able to impose static inclined eccentricity on the rotor, a special test bed was built. The stator and the rotor bearings at the two ends of the motor were separately mounted on the test bed. This made it possible to displace any of bearings separately and create different static inclined eccentricities. By this manner, the salient pole machine with different types and degrees of static inclined eccentricities can be provided for tests. As shown in Fig. 11, a clock was provided to check the correct position of bearings. A selectable resistance load at machine terminals has been used to obtain a variable load on the machine.
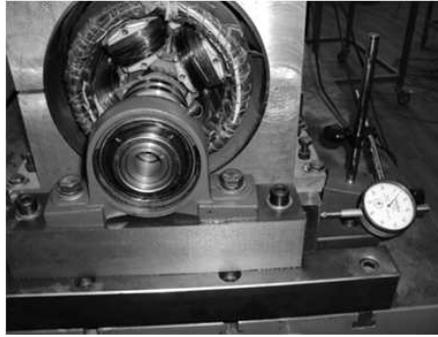
Figure 11. A clock for checking the correct position of bearings.

To obtain the mutual inductance between stator phase A and stator phase B, a sinusoidal voltage was applied in stator phase A and the voltage induced in the stator phase B was measured as a function of the rotor position. The mutual inductance was calculated as follows:

$$L_{AB}\left(\theta\right) = \frac{V_B(\theta)}{V_A(\theta)} L_{AA}(\theta) \tag{41}$$

where $V_A(\theta)$ and $V_B(\theta)$ are induced voltages in stator phase A and stator phase B, respectively and $L_{AA}(\theta)$ is self inductance of stator phase A, previously calculated by means of phase A voltage and current measurements.

The induced voltage in phase A was derived as follows:

$$V_A = \sqrt{V_s^2 - \left(r_A i_A\right)^2} \tag{42}$$

where V_s is the applied voltage, i_A is the current following in stator phase A and r_A is stator phase A resistance ($1.36\,\Omega$). To avoid the magnetic saturation, a low ac voltage was applied. The phase A voltage drop was negligible in the experiments.

Figure 12 shows the mutual inductance under axial eccentricity condition for the experiment and simulation. It is apparent that the inductance profiles coming from the simulation and experiment demonstrate a satisfactory match.

The percentage increase in the stator current harmonics due to static inclined eccentricity has been summarized in Table 3. It is obvious again that the 19th stator current harmonic has the highest relative percentage increase.

As shown in Tables 2–3, cases with low average SE demonstrate similar amplitude of 19th stator current harmonic as in the healthy case. Thus, these cases will be difficult to identify with machine current

(a)   (b)
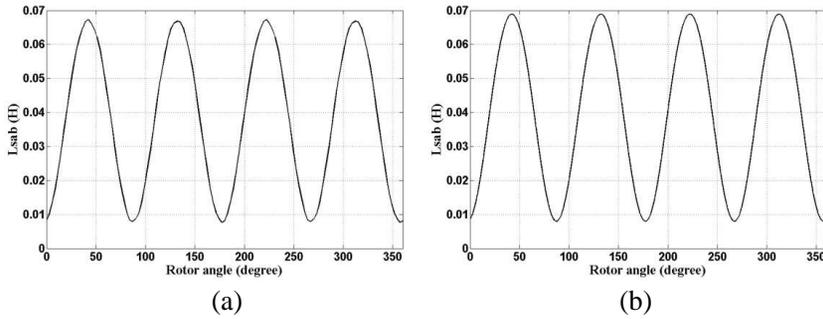
Figure 12. Mutual inductance between stator phase A and stator phase B under static inclined eccentricity (one end is 20% SE and the other end is 80% SE) for the (a) experiment and (b) simulation.

Table 3. Experimental relative percentage increase of stator current harmonics due to different inclined eccentricities under 50% load level.

Harmonic order	(SE degree (%) at two ends)				
	−30 +30	−60 +60	−20 +60	+30 +60	+70 +70
5th	0%	1%	5%	5%	6%
7th	0%	0%	4%	4.5%	7%
11th	0%	0.5%	3%	4%	5.5%
13th	0%	1%	4%	10%	14%
17th	0%	0.5%	3.5%	11%	15%
19th	0.5%	2%	16%	43%	57%
23th	1%	1%	7%	19%	23%

analysis. Other techniques such as temperature and bearing vibration analysis may therefore have to be used in these cases for fault detection.

The percentage increase in the 19th stator current harmonic due to static inclined eccentricity under different load levels for the experiment and simulation has been summarized in Table 4. As shown, under no-load condition, the amplitude of this harmonic is less sensitive to the severity of eccentricity. Therefore, the 19th stator current harmonic of the loaded machine can be applied for inclined eccentricity detection.

Air gap nonuniformity results in an asymmetric air gap flux distribution. Flux space harmonic components move in the air gap relative to the stator and therefore induce corresponding current

Table 4. Relative percentage increase of 19th stator current harmonic due to different inclined eccentricities under different load levels for the experiment (Exp.) and simulation (Sim.).

Load level	(SE degree (%) at two ends)				
	−30 +30	−60 +60	−20 +60	+30 +60	+70 +70
0% (Sim.)	0%	1%	19%	41%	61%
50% (Sim.)	2%	3%	24%	58%	80%
100% (Sim.)	1%	3%	26%	61%	85%
0% (Exp.)	1%	1%	7%	28%	33%
50% (Exp.)	0.5%	2%	16%	43%	57%
100% (Exp.)	1%	1%	20%	44%	59%

harmonics in the stator phases. These space harmonic components will increase as air gap nonuniformity increases and consequently the amplitude of stator current harmonics increases further. The 17th and 19th stator current harmonics have been noticed and discussed in [19] and [21] as radial eccentricity indicators in a four pole salient pole synchronous machine. Simulation and experimental results in the present paper show that the 19th stator current harmonic can be used for axial nonuniformity detection in a four pole salient pole machine.

Figure 13 shows variation of the amplitude of 19th stator current harmonic as percentage values versus average eccentricity level for the experiment and simulation. The main reason for the difference between simulation and experimental results is due to neglecting the magnetic saturation. Magnetic saturation limits the asymmetry of the flux distribution, caused by nonuniform air gap, and puts an upper limit on the amplitude of current harmonics. The magnetic saturation also puts an upper limit on the unbalanced magnetic pull (UMP) [29]. Few efforts have been made to add the magnetic saturation effects in the modeling process of winding function approach [30, 31]. Saturation results in flux space harmonic components traveling in the air gap with the synchronous speed. All available techniques based on WFA, model the saturation effect by a proportional increase in the air gap length, considering only fundamental and third flux pace harmonic components. The authors plan to incorporate the magnetic saturation in the simulation, using more realistic model.

The proposed method is based on an extension of winding function theory to 3D. The only information required in this theory is the winding layout and machine geometry. This theory has no restriction
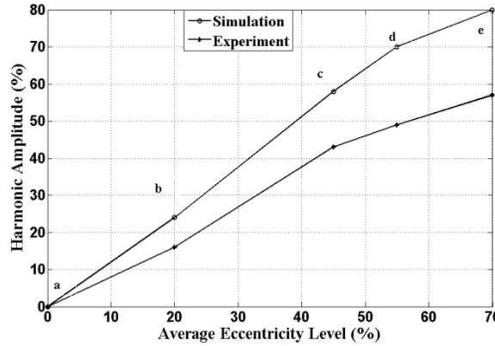
Figure 13. Relative percentage increase of 19th stator current harmonic versus average eccentricity level for the experiment and simulation. Test points are (a) healthy, (b) −20%, +60%, (c) +30%, +60%, (d) +40%, +70% and (e) uniform 70%.

about the power of machine. For example in [19], this theory has been applied for centricity detection in 475 kw synchronous generator. Therefore, the proposed method in the present paper can be applied for performance analysis of any faulty salient pole synchronous machine with any type of air gap and winding distribution, while taking into account all spatial and time harmonics.

8. CONCLUSION

For the calculation of salient pole machine inductances under radial and axial non-uniformity conditions, the modified winding function method is extended to 3D. Developed method considers the variation of the mean radius function, while in previous studies, based on MWFA, the geometrical model of salient pole machines has been simplified and this function has been considered to be constant. Detailed inductance equation derivation and modeling procedures have been presented. The extended theory will be particularly helpful in the study of salient pole machines with radial and axial non-uniform air gap such as that caused by inclined eccentricity. For analysis of different static inclined eccentricities, a precise geometrical model of machine under these conditions is presented. The mutual inductance profiles obtained from the simulation and experiment demonstrate a satisfactory mach. Simulation and experimental results show that the 19th stator current harmonic of the loaded machine can be employed to detect the static inclined eccentricity in salient pole machine. Also, it was shown that the inclined eccentricities symmetric to the midpoint of the machine

shaft are difficult to identify with motor current signature analysis and a different technique has to be used.

REFERENCES

1. Faiz, J. and B. M. Ebrahimi, "Mixed fault diagnosis in three-phase squirrel-cage induction motor using analysis of air-gap magnetic field," *Progress In Electromagnetics Research,* Vol. 64, 239–255, 2006

2. Nandi, S., H. Toliyat, and X. Li, "Condition monitoring and fault diagnosis of electrical motors: A review," *IEEE Transactions on Energy Conversion*, Vol. 20, No. 4, 719–729, 2005.

3. Torkaman, H. and E. Afjei, "FEM analysis of angular misalignment fault in SRM magnetostatic characteristics," *Progress In Electromagnetics Research*, Vol. 104, 31–48, 2010.

4. Li, X. and S. Nandi, "Performance analysis of a three phase induction machine with inclined static eccentricity," *IEEE Transactions on Industry Application*, Vol. 43, No. 2, Mar. 2007.

5. Meshgin-Kelk, H., J. Milimonfared, and H. Toliyat, "Interbar currents and axial fluxes in healthy and faulty induction motors," *IEEE Transactions on Industry Applications*, Vol. 40, No. 1, 128–134, 2004.

6. Faiz, J. and B. M. Ebrahimi, "Static eccentricity fault diagnosis in an accelerating no-load three-phase saturated squirrel-cage induction motor," *Progress In Electromagnetics Research B*, Vol. 10, 35–54, 2008.

7. Vaseghi, B., N. Takorabet, and F. Meibody-Tabar, "Transient finite element analysis of induction machines with stator winding turn fault," *Progress In Electromagnetics Research,* Vol. 95, 1–18, 2009.

8. Torkaman, H. and E. Afjei, "Hybrid method of obtaining degrees of freedom for radial air gap length in SRM under normal and faulty conditions based on magnetostatic model," *Progress In Electromagnetics Research*, Vol. 100, 37–54, 2010

9. Faiz, J., B. M. Ebrahimi, and M. B. B. Sharifian, "Time stepping finite element analysis of rotor broken bars fault in a three-phase squirrel-cage induction motor," *Progress In Electromagnetics Research,* Vol. 68, 53–70, 2007.

10. De Bortoli, M. J., S. J. Salon, and C. J. Slavic, "Effect of rotor eccentricity and parallel winding on induction behavior: A study using finite element analysis," *IEEE Transactions on Magnetics*, Vol. 29, No. 2, 1676–1682, 1993.

11. Toliyat, H., T. A. Lipo, and J. C. White, "Analysis of a concentrated winding induction machine for adjustable speed drive applications, part-1 (motor analysis)," *IEEE Transactions on Energy Conversion*, Vol. 6, 679–692, 1991.

12. Toliyat, H. and T. A. Lipo, "Transient analysis of cage induction machines under stator, rotor bar and end-ring faults," *IEEE Transactions on Energy Conversion*, Vol. 10, No. 2, 241–247, Jun. 1995.

13. Milimonfared, J., H. M. Kelk, A. D. Minassians, S. Nandi, and H. A Toliyat, "A novel approach for broken bar detection in cage induction motors," *IEEE Transactions on Industry Applications*, Vol. 35, 1000–1006, 1999.

14. Luo, X., Y. Liao, H. Toliyat, and T. A. Lipo, "Multiple coupled circuit modeling of induction machines," *IEEE Transactions on Industry Applications*, Vol. 31, 311–318, 1995.

15. Joksimovic, M. G. and J. Penman, "The detection of inter turn short circuits in the stator windings of operating motors," *IEEE Transactions on Industry Application*, Vol. 47, 1078–1084, 2000.

16. Al-Nuim, N. A. and H. Toliyat, "A novel method for modeling dynamic air-gap eccentricity in synchronous machines based on modified winding function theory," *IEEE Transactions on Energy Conversion*, Vol. 13, 156–162, 1998.

17. Faiz, J. and I. Tabatbaei, "Extension of winding function theory for non-uniform air gap in electric machinery," *IEEE Transactions on Magnetics*, Vol. 38, No. 6, Nov. 2002.

18. Bossio, G., C. D. Angelo, J. Solsona, G. Garcia, and M. I. Valla, "A 2-D model of the induction machine: An extension of the modified winding function approach," *IEEE Transactions on Energy Conversion*, Vol. 19, No. 1, Mar. 2004.

19. Tabatabaei, I., J. Faiz, H. Lesani, and M. T. Nabavi-Razavi, "Modeling and simulation of a salient pole synchronous generator with dynamic eccentricity using modified winding function approach," *IEEE Transactions on Magnetics*, Vol. 40, No. 3, May 2004.

20. Joksimovic, G. M., "Dynamic simulation of cage induction machine with air gap eccentricity," *IEE Proc. Electr. Power Appl.*, Vol. 152, No. 4, 803–811, Jul. 2005.

21. Faiz, J., B. M. Ebrahimi, and M. Valavi, "Mixed eccentricity fault diagnosis in salient pole synchronous generator using modified winding function method," *Progress In Electromagnetics Research B*, Vol. 11, 155–172, 2009.

22. Akbari, H., J. Milimonfared, and H. Meshgin-Kelk, "Axial static eccentricity detection in induction machines by wavelet technique," *International Review of Electrical Engineering,* Vol. 5, No. 3, 2010.

23. Joksimovic, G. M., M. Durovic, J. Penman, and N. Arthur, "Dynamic simulation of dynamic eccentricity in induction machines-winding function approach," *IEEE Transactions on Energy Conversion*, Vol. 15, No. 2, 143–148, 2000.

24. Nandi, S., "Modeling of induction machines including stator and rotor slot effects," *IEEE Transactions on Industry Applications,* Vol. 40, No. 4, 2004.

25. Ojaghi, M. and J. Faiz, "Extension to multiple coupled circuit modeling of induction machines to include variable degrees of saturation effects," *IEEE Transactions on Magnetics*, Vol. 44, No. 11, 2008.

26. Akbari, H., H. Meshgin-Kelk, and J. Milimonfared, "Induction machine modeling including the interbar currents using winding function approach," *International Review of Electrical Engineering*, Vol. 4, No. 2, 2009.

27. Ostovic, V., *Computer Aided Analysis of Electrical Machines, A Mathematical Approach*, Prentice Hall, 1994.

28. Rahimian, M. and K. Butler-Purry, "Modeling of synchronous machines with damper windings for condition monitoring," *International Electric Machines and Drives Conference, IEMDC 2009*, Miami, Florida, USA, 2009.

29. Perers, R., U. Lunin, and M. Leijon, "Saturation effects on unbalanced magnetic pull in a hydroelectric generator with an eccentric rotor," *IEEE Transactions on Magnetics*, Vol. 43, No. 10, 2007.

30. Nandi, S., "A detailed model of induction machine with saturation extendable for fault analysis," *IEEE Transactions on Industry Application*, Vol. 40, No. 5, 1302–1309, 2004.

31. Babaei, M., J. Faiz, B. M. Ebrahimi, S. Amini, and J. Nazarzadeh, "A detailed analytical model of a salient-pole synchronous generator under dynamic eccentricity fault," *IEEE Transactions on Magnetics*, Vol. 99, 2011.